

ASPS Performance with Large Payloads Onboard the Shuttle Orbiter

Claude R. Keckler*

NASA Langley Research Center, Hampton, Va.

An analysis has been conducted, using a high-fidelity digital computer simulation, to establish the viability of the Annular Suspension and Pointing System (ASPS) in satisfying the pointing and stability requirements of facility class payloads, such as the Solar Optical Telescope (SOT) (6600 kg mass), when subjected to the orbiter disturbance environment. The ASPS, which utilizes a combination of magnetic bearing actuators and conventional gimbals, was found to be readily capable of isolating the payload from the orbiter disturbances, and of satisfying the payload's pointing and stability requirements without having to resort to an orbiter free-drift mode. Description of the ASPS hardware and system simulation is presented along with analysis results demonstrating the applicability of ASPS to large payloads.

Nomenclature

ASPS	= Annular Suspension and Pointing System
AVS	= ASPS vernier system
c.m.	= center of mass
DRIRU-II	= Dry Rotor Inertial Reference Unit-II
LOS	= line of sight
MBA	= magnetic bearing actuator
MJA	= mounting/jettison assembly
NSSC-II	= NASA Standard Spacecraft Computer-II
SOT	= solar optical telescope
VRCS	= vernier reaction control system

Introduction

PROJECTED payloads for the Shuttle era include a number of experiments which require pointing and stabilization far in excess of the Shuttle orbiter capabilities. In addition, these requirements must be satisfied for extended viewing periods (up to 1 h), and thus in the presence of carrier vehicle disturbances. The disturbances imparted to the orbiter and its cargo are a result of crew activity and/or VRCS thruster firings for spacecraft attitude hold, in addition to the less severe orbital environment forces and torques. To satisfy the pointing and stability requirements of the various postulated payloads, numerous approaches have been proposed, including the use of auxiliary pointing systems.

The most promising candidate auxiliary pointing system for these applications is the ASPS. The ASPS utilizes MBA's in conjunction with a pair of conventional gimbals to permit high accuracy pointing and stabilization, as well as acquisition and tracking of desired targets. Previous simulation studies of ASPS performed by NASA Langley and JPL^{1,2} have shown its applicability in satisfying the mission requirements of small experiments (up to 600 kg). However, the desirability of having a pointing system capable of satisfying the requirements of a large variety of payloads becomes readily obvious in terms of development and operational costs. Therefore, an investigation was undertaken, using a multi-degree-of-freedom simulation of the ASPS, Shuttle orbiter, and payload, to define the performance of this pointing system with a large payload (6600 kg) during periods of VRCS firings and crew motions.

ASPS Description

The ASPS (Fig. 1) is comprised of the following major electromechanical subassemblies: 1) vernier system, 2) lateral and elevation gimbal assemblies, and 3) mounting/jettison assembly.

The AVS consists of a payload plate attached to an L-shaped rotor. This combination is suspended on five MBA's, three axial and two radial MBA's. These MBA's are used to provide control of rotor motion in three translational and two rotational degrees-of-freedom, and have a force capacity of 33.9 N for each axial MBA, and 14.2 N for each radial MBA. These two rotations, about axes in the plane of the rotor, are defined as pitch and yaw. The third rotation, about an axis perpendicular to the plane of the rotor, is defined as roll, and is controlled by a segmented ac induction motor. Rotor position in the MBA gaps is determined by proximeters, while a resolver is used to establish roll position. Data transmission to and from the payload is performed through the use of a multichannel optical coupler. Power to the equipment mounted on the payload plate is supplied via a rotary transformer. Therefore, since no contacting elements are used between the fixed and suspended portions of the vernier system, the payload is essentially a constrained free-flyer, and thus isolated from orbiter disturbances.

The AVS is mounted on a pair of conventional gimbals, each employing a brushless dc torquer of 33.9 Nm capacity, and resolvers for commutation and gimbal angle information. Signals and power are passed through the gimbals by means of flex capsules. The gimbals are utilized for system deployment from the caged position after attaining orbit, for target acquisition, tracking, and slewing to a new target. The gimbals also function as a backup system for continuation of the experiment's operation, at reduced performance levels, should it be necessary to turn off the AVS.

The interface structure between the gimbals/AVS combination and the payload bay integration platform is provided by the MJA. The MJA contains the separation mechanism necessary to unload the gimbal bearings from payload induced vibrations during launch and landing. In addition, pyrotechnic devices are included in the MJA to permit the release of the pointing system, and its payload, from the carrier vehicle should an emergency situation arise.

The ASPS utilizes the NSSC-II and associated software as its digital controller. In addition, several electronics assemblies are provided as part of the system. Payload attitude is provided by whatever sensor (e.g., sun sensor, star tracker, etc.) is appropriate for the particular mission, or directly by the payload itself.

Presented as Paper 80-1779 at the AIAA Guidance and Control Conference, Danvers, Mass., Aug. 11-13, 1980; submitted Oct. 24, 1980; revision received June 19, 1981. This paper is declared a work of the U.S. Government and therefore is in the public domain.

*Aero-Space Technologist, Stability and Control Branch, FDCD. Member AIAA.

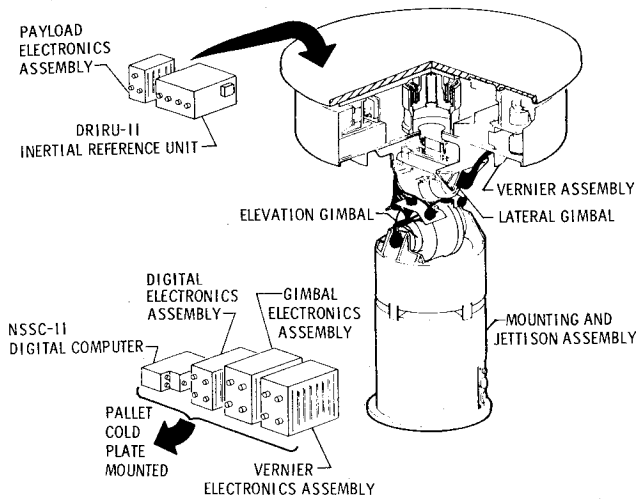


Fig. 1 Annular Suspension and Pointing System (ASPS) concept.

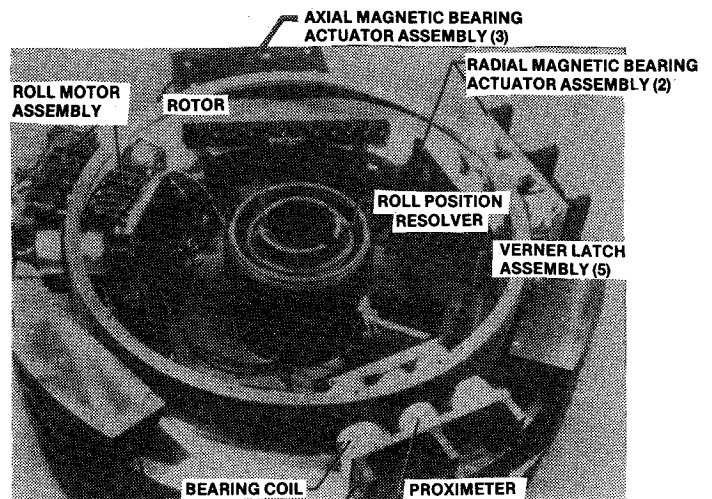


Fig. 2 ASPS vernier system hardware.

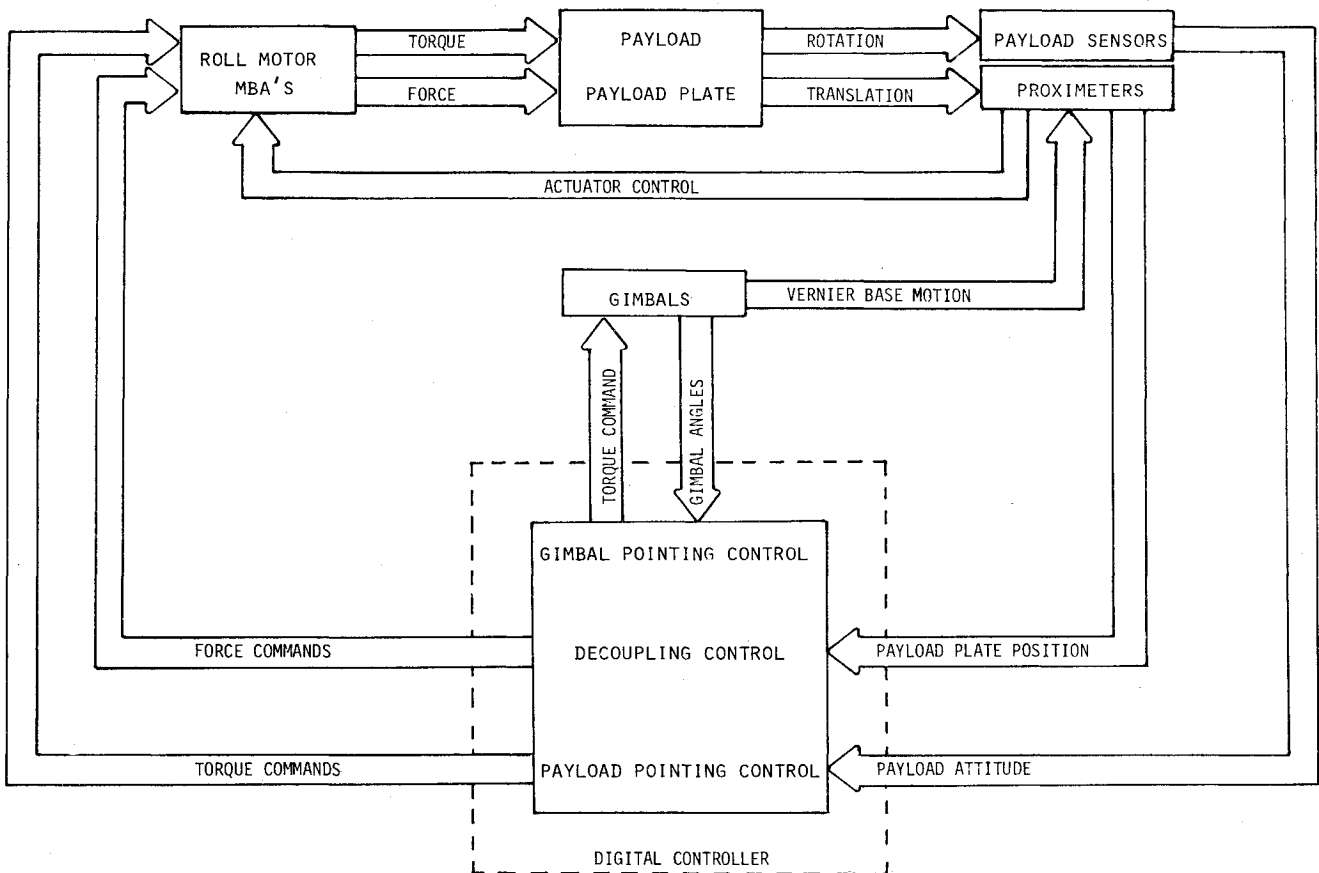


Fig. 3 Block diagram of ASPS control loops.

A more detailed description of the ASPS design is contained in Ref. 3.

The AVS hardware has been fabricated, assembled, and is undergoing laboratory evaluation. A photograph of that hardware is shown in Fig. 2. In addition, several other ASPS components have been fabricated (e.g., gimbal drive assembly, flex capsule, optical coupler, etc.), and have been subjected to thorough bench tests. Results from these tests were used to generate the math models used in the computer simulation.

The ASPS utilizes several combinations of control loops to accomplish its various assigned tasks. These combinations are determined by the selected operational modes, i.e., fine pointing, slewing, etc. The control and sensing loops

associated with the fine pointing task, which is the subject of this study, are schematically represented in Fig. 3.

There are three principal control loops in operation during the fine pointing task. The payload pointing control loop utilizes payload sensor information to generate vernier actuator (roll motor and MBA's) torques and forces, which act on the payload/payload plate combination, thus maintaining the desired orientation. Proximeter signals, indicating the position of the AVS rotor in the MBA gaps, are used by the decoupling control loop to generate axial and radial forces to maintain the AVS rotor translationally centered. These translational forces act through the c.m. of the AVS rotor/payload plate/payload mass to avoid payload pointing control loop errors. This feed-forward control loop concept provides the

ASPS with the flexibility of an end-mount payload pointer, and the performance of c.m. attached system. The proximity signals are also used to generate commands to the gimbal pointing control loops to null the relative angular deviation between the gimbal assemblies and the AVS, thus keeping the AVS rotor centered between MBA pole faces.

Payload Description

Previous studies of the ASPS considered its applicability only to small payloads (up to 600 kg). However, since it is highly desirable in terms of resources expenditures and operational standardization, to have a single system capable of satisfying a large range of requirements, it was decided to examine the system's performance capability when supporting large payloads. The largest proposed payload was selected for this investigation. The largest known contemplated experiment, to date, is the SOT being developed by NASA Goddard Space Flight Center, and shown in Fig. 4. The configuration, shown herein, is 3.8 m in diameter and 7.3 m long, and is comprised of a number of separate instruments for use by several principal investigators. This configuration has a total mass of 6600 kg and has a 3.44 m c.m. offset from the bottom of the experiment along the LOS.

Stability requirements for the scientific experiments of SOT have been specified as 0.08 arc-sec, with viewing periods of up to 1 h. To attempt to satisfy these requirements through the restriction of crew activity and/or a free-drift mode of operation for extended periods does not appear reasonable if other Shuttle experiments are to be accommodated. Thus, it becomes essential that the pointing system be capable of satisfying payload control requirements in the presence of carrier vehicle disturbance.

Analysis Conditions and Results

The performance of the ASPS, with an SOT size payload, mounted in the Shuttle orbiter payload bay was evaluated to establish the impact of external disturbances on the system during periods when stringent control requirements must be satisfied. The analysis tool used in this effort is a multi-degree-of-freedom, digital computer simulation of the ASPS, its payload, and the Shuttle orbiter. This simulation encompasses the rigid body dynamics of the orbiter, the pointing system, and the payload, and, where applicable, mathematical models of various components such as MBA's, ASPS sensors, and digital controller, based on actual hardware data.

During the course of the MBA characterization and calibration, it was shown that this actuator was capable of responding to input commands as low as 0.02 arc-sec. From these data, a mathematical representation of the MBA was generated, which duplicated the measured performance. However, since the command resolution limit was a result of the test environment and measuring equipment, it was not included in the math model of the actuator. It was, instead, replaced by the resolution limit represented by the granularity of the 12-bits digital-to-analog (D/A) converter of the digital controller.³ As in the hardware, the model of the MBA was also provided with dual output force ranges, e.g., 33.9 N for normal operation and 0.34 N for fine pointing in the case of the axial MBA's. This, therefore, resulted in quantization levels of 8.28×10^{-3} N and 8.3×10^{-5} N respectively. Similar scaling was used for the radial MBA's.

The sensing element of the MBA, namely, the proximity sensor for determining rotor position was modeled with an accuracy of 0.001 mm. Noise characteristics for this sensor were not included in this study, since, in Ref. 2, it was pointed out that when modeled as band-limited white noise with a bandwidth of 50 Hz, these characteristics were found to have no effect on system stability. In previous work by Sperry, it was demonstrated that the contribution to system stability error

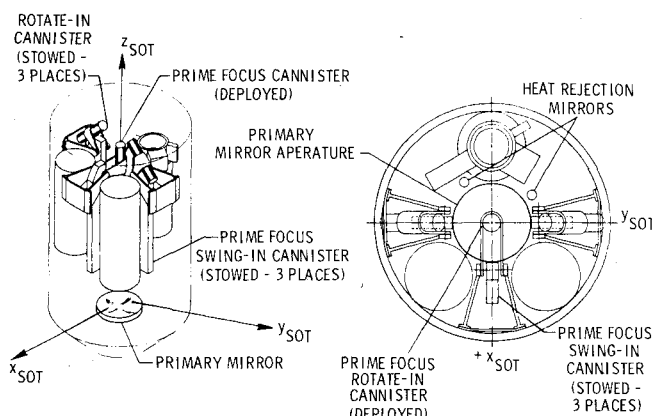


Fig. 4 Solar Optical Telescope (SOT) concept.

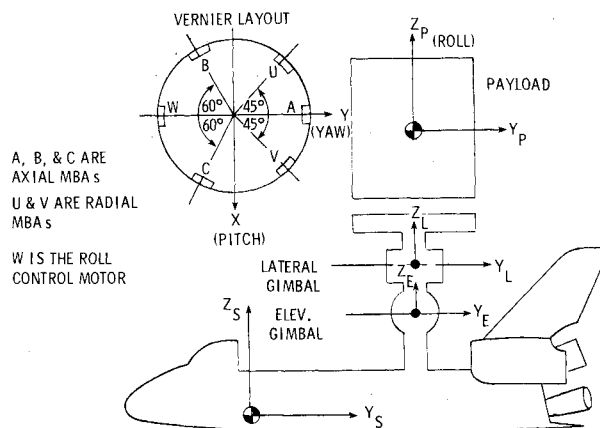


Fig. 5 Definition of coordinate systems.

from the gimbal torquer anomalies (e.g., friction, hysteresis, cogging) was only 10^{-6} arc-sec. Thus, the gimbal assemblies were not modeled in this study.

The digital controller was represented by introducing transport lags of 4 ms in the control loop. The payload sensors, i.e., the DRIRU-II and the sun sensor or payload provided signals, were assumed as ideal sensors since it was desired to verify that the pointer was sensor limited in performance for these large payloads, as it had been for the smaller payloads.¹

The geometrical relationships of the various elements and their attendant coordinate systems are schematically represented in Fig. 5. The ASPS and its payload are located aft and above the Shuttle orbiter c.m. as follows:

$$Y_s = 2.2 \text{ m aft of Shuttle c.m.}$$

$$Z_s = 0.75 \text{ m above Shuttle c.m.}$$

The system and its payload were subjected to disturbances resulting from VRCS thruster firings. The distribution of these thrusters and their output on the orbiter are shown in Table 1. (Note E-4 and E+6 on Table 1 denote 10^{-4} and 10^6 , respectively.) Using the simulation, a survey was conducted to identify which combination of VRCS thruster firings and pointing system gimbal orientations provided the most severe impact on the system's performance. The data from that survey, presented in Ref. 4, indicated that the maximum impact resulted from a pitch or roll axis VRCS firing. The gimbal angles, or payload look angle, which placed maximum demands on ASPS performance for these disturbances are -86 deg elevation and 0 deg lateral for pitch disturbances and 0 deg elevation and -40 deg lateral for roll disturbances.

Table 1 Shuttle VRCS configuration and characteristics

Axis	Burn time, s	VRCS angular acceleration, rad/s ²	VRCS translational acceleration, m/s ²			Thrusters operating
			\ddot{X}_s	\ddot{Y}_s	\ddot{Z}_s	
Y_s roll (+)	0.20	$+6.215E-4$	$+0.002176$	0	$+0.002318$	2,4,6
X_s pitch (+)	0.52	$+2.918E-4$	0	0	$+0.00263$	5,6
Z_s yaw (+)	0.48	$+2.920E-4$	-0.0004518	0	$+0.001004$	2,3

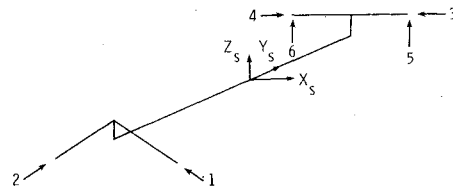
STS-1 mass properties:

Mass = 5790 slugs = 84,562 kg

$I_x = 6.282E+6$ slug-ft² = $8.524E+6$ kg-m²

$I_y = 0.809E+6$ slug-ft² = $1.098E+6$ kg-m²

$I_z = 6.544E+6$ slug-ft² = $8.879E+6$ kg-m²

Table 2 ASPS response to crew motion and VRCS disturbance ($\sigma = -86$ deg, $\gamma = 0$ deg)

Disturbance	Max. $A_{\perp LOS}$, m/s ²		Max. MBA force, N					Max. gim. torque, Nm		Max. ptg. error, arc-sec	
	At lat. gim.	At P/L	A	B	C	U	V	T_o	T_γ	ϕ	θ
Crew motion + Pitch	0.00086	0.000069	2	-2.8	0.9	0.3	-0.7	1.2	-1.2	-0.0006	-0.0015
VRCS with crew motion	0.00447	0.000477	19.8	-12	-8	-2	-2.6	12	-1.2	-0.005	-0.0015

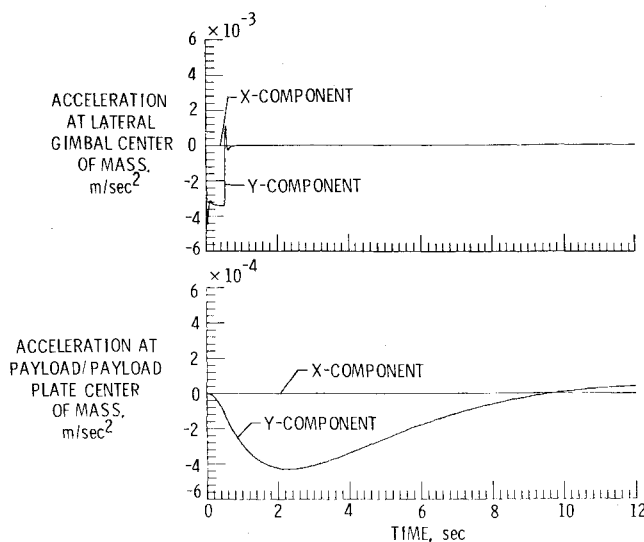


Fig. 6 Acceleration perpendicular to LOS measured at the lateral gimbal and payload/payload plate c.m. (initial conditions: $\sigma = -86$ deg, $\gamma = 0$ deg).

Figure 6-8 present time histories of the impact of a pitch VRCS disturbance on ASPS and its payload, and the resultant pointing system's performance under that disturbance environment. These curves are typical system-time histories, and are representative of ASPS capability while supporting a large payload onboard the Shuttle orbiter. As can be noted from these figures, the system was set at its worst payload orientation as determined by the survey of Ref. 4. Although large payloads, such as SOT, require a viewing angle of only 60 deg from the vertical (Z_p in Fig. 5), it was decided to evaluate ASPS performance at the worst orientation. If the pointer could meet the control requirements under these conditions, then it could thus readily satisfy the requirements of like-payloads having smaller viewing angles, since, in general, the smaller the gimbal angle, the smaller the impact of the disturbances.

As can be seen from Fig. 6, the effect of the pitch VRCS disturbance on the payload, when compared with its impact on the lateral gimbal, was attenuated by approximately an

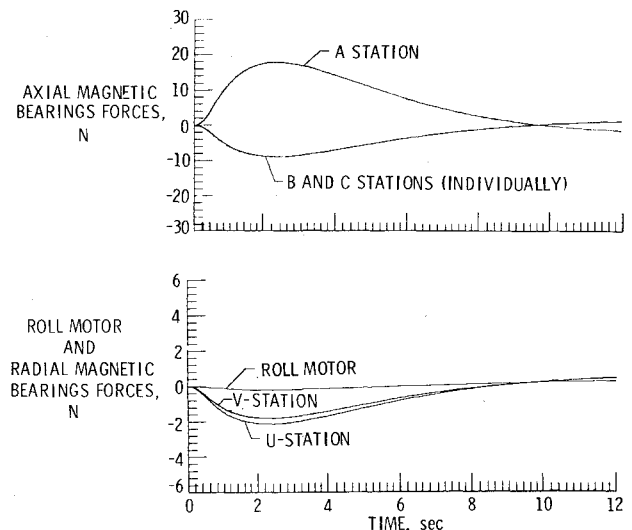


Fig. 7 Magnetic bearing actuators and roll motor forces (initial conditions: $\sigma = -86$ deg, $\gamma = 0$ deg).

order of magnitude (note scale change between top and bottom graphs of Fig. 6). This is attributable to the AVS isolation capability. From Fig. 7, it can be noted that the maximum force required from the axial MBA's to control the pitch VRCS disturbance was 18 N, while the maximum demand placed on the radial MBA's was for a control force of about 2 N. This compares favorably with the capacity of these actuators, and indicates that the magnetic suspension system is adequately sized to support large payloads. In addition, the maximum control torque required from the system gimbals (Fig. 8) represents 30% of their capacity. Finally, Fig. 8 indicates the maximum pointing error experienced during this period was less than 0.005 arc-sec (0.00447 arc-sec in the computer printout) which, in the case of SOT, represents approximately 5.6% of the allowable pointing error of 0.08 arc-sec as specified by the experiment. The limit cycle experienced after the disturbance had been removed was found to be, from the printout, 7×10^{-5} arc-sec peak-to-peak with about a 5 Hz frequency.

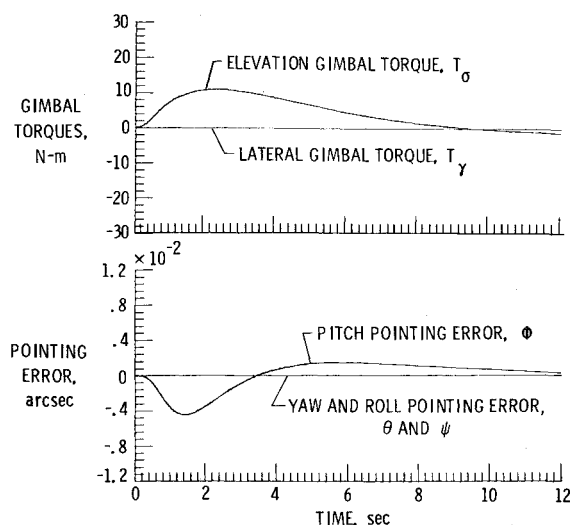


Fig. 8 Gimbal torques and payload pointing errors (initial conditions: $\sigma = -86$ deg, $\gamma = 0$ deg).

Since this pointing system is to operate onboard a manned vehicle, its performance while being subjected to crew motions, as well as to combined crew motions and VRCS firings, was examined. Typical results from this examination are presented in Table 2. It was found that the dominating disturbance onboard the orbiter resulted from VRCS firings and that crew motions contributed little to the system's pointing errors. Peak errors resulting from combined crew motion and VRCS disturbance represented about 6.2% of the specified allowable error.

The pointing errors resulting from VRCS thruster firings and crew motions, as demonstrated by Fig. 8 and Table 2, are

3-sigma values, and representative of the system's expected capability with large payloads in the Shuttle operational environment.

Concluding Remarks

Using a digital computer simulation, an analysis was conducted to determine the performance capability of the Annular Suspension and Pointing System in satisfying large payload requirements, as exemplified by the Solar Optical Telescope, while onboard the Shuttle orbiter. The pointing system and its payload were subjected to disturbances resulting from crew motions in the orbiter aft flight deck and vernier reaction control system firings. Peak pointing errors of about 0.005 arc-sec were experienced under the disturbance environment simulated in this effort. In the case of the SOT, this is well within the 0.08 arc-sec requirements specified by the payload. Based on these results, it is concluded that the ASPS presented an attractive approach for satisfying large payload mission requirements. Utilization of such a pointing system can allow for simultaneous operation of facility class payloads and experiments relying on orbiter control.

References

- Anderson, W.W., Groom, N.J., and Woolley, C.T., "Annular Suspension and Pointing System," *Journal of Guidance and Control*, Vol. 2, Sept.-Oct. 1979, pp. 367-373.
- "Space Shuttle Experiment Pointing Mount (EPM) Systems: An Evaluation of Concepts and Technologies," Vol. II, Jet Propulsion Laboratory, Report 701-1, April 1, 1977.
- Cunningham, D.C., Gismondi, T.P., and Wilson, G.W., "System Design of the Annular Suspension and Pointing System (ASPS)," *Proceedings of the AIAA Guidance and Control Conference*, Palo Alto, Calif., Aug. 7-9, 1978.
- Keckler, C.R., Kibler, K.S., and Rowell, L.F., "Determination of ASPS Performance for Large Payloads in the Shuttle Orbiter Disturbance Environment," NASA TM-80136, Oct. 1979.

From the AIAA Progress in Astronautics and Aeronautics Series

SPACE SYSTEMS AND THEIR INTERACTIONS WITH EARTH'S SPACE ENVIRONMENT—v. 71

Edited by Henry B. Garrett and Charles P. Pike, Air Force Geophysics Laboratory

This volume presents a wide-ranging scientific examination of the many aspects of the interaction between space systems and the space environment, a subject of growing importance in view of the ever more complicated missions to be performed in space and in view of the ever growing intricacy of spacecraft systems. Among the many fascinating topics are such matters as: the changes in the upper atmosphere, in the ionosphere, in the plasmasphere, and in the magnetosphere, due to vapor or gas releases from large space vehicles; electrical charging of the spacecraft by action of solar radiation and by interaction with the ionosphere, and the subsequent effects of such accumulation; the effects of microwave beams on the ionosphere, including not only radiative heating but also electric breakdown of the surrounding gas; the creation of ionosphere "holes" and wakes by rapidly moving spacecraft; the occurrence of arcs and the effects of such arcing in orbital spacecraft; the effects on space systems of the radiation environment, etc. Included are discussions of the details of the space environment itself, e.g., the characteristics of the upper atmosphere and of the outer atmosphere at great distances from the Earth; and the diverse physical radiations prevalent in outer space, especially in Earth's magnetosphere. A subject as diverse as this necessarily is an interdisciplinary one. It is therefore expected that this volume, based mainly on invited papers, will prove of value.

737 pp., 6 × 9, illus., \$30.00 Mem., \$55.00 List

TO ORDER WRITE: Publications Dept., AIAA, 1290 Avenue of the Americas, New York, N.Y. 10104